IEEE Access
Multidisciplinary | Rapid Review | Open Access Journal

Received March 3, 2019, accepted March 26, 2019, date of publication April 2, 2019, date of current version April 16, 2019.

Digital Object Identifier 10.1109/ACCESS.2019.2908877

An Effective Numerical Control Machining Process Optimization Approach of Part With Complex Pockets for Numerical Control Process Reuse

BO HUANG[1], SHUSHENG ZHANG[1], RUI HUANG[2], XIULING LI[1,3], YAJUN ZHANG[1], AND JIACHEN LIANG[1]

[1]The Key Laboratory of Contemporary Designing and Integrated Manufacturing Technology, Ministry of Education, Northwestern Polytechnical University, Xi'an 710072, China
[2]College of IOT Engineering, Hohai University, Changzhou 213022, China
[3]Zhengzhou Railway Vocational & Technical College, Zhengzhou 450052, China

Corresponding author: Shusheng Zhang (zssnwpu@163.com)

This work was supported in part by the National Science Foundation of China under Grant 51875474 and Grant 51605142, and in part by the Equipment Pre-Research Domain Foundation of China under Grant 61409230102.

ABSTRACT Recently, various process reuse technologies have come to be widely used in manufacturing. The existing methods mainly focus on searching and reusing similar NC processes. For the optimization of process schemes generated by reusable NC machining processes, however, no effective strategy has yet been proposed, especially when it comes to complex parts with intersecting features. To address this issue, we present, here, an effective NC machining process optimization approach of the part with complex pockets for NC process reuse. This approach involves two levels, that of the machining feature and that of the part. In the former case, the cutting tool and a cutting depth of the machining region is first optimized by making full use of the tool's machining capacity and avoiding air-cutting. In the latter case, the cutting sequence of the machining regions is further optimized in the macro process so as to maintain the efficiency of the process scheme. The effectiveness of the proposed approach is verified by a jag of the electronic product and an aircraft structural in our developed prototype system based on CATIA. The presented method can be integrated into commercial CAD/CAM software for rapid NC programming.

INDEX TERMS NC process reuse, machining region, feature-based NC machining, NC machining process optimization.

NOMENCLATURE

NC	Numerical control
CAM	Computer-aided manufacturing
CAD	Computer-aided design
ACO	Ant colony optimization
TS	Tabu search
GA	Genetic algorithm
SA	Simulated annealing

I. INTRODUCTION

With the evolution of manufacturing toward new-generation intelligent manufacturing, various countries have proposed many manufacturing industry promotion projects, such as Germany's ''Industry 4.0'', ''China Manufacturing 2025'', and the United States' ''Industry Internet +''. In this dynamic and competitive environment, the constant upgrading of industry poses new challenges when it comes to high-quality and efficient manufacturing [1]. Meanwhile, NC machining, as the main means of producing complex products, is imposing new requirements for high-efficiency and intelligence level of NC machining process planning technology, especially for small-batch products, such as the jig of electronic product and the aircraft structural. Powerful CAM systems have recently come into wide use, but the various aspects of process analysis and decision-making continue to depend largely on the knowledge and experience of designers. Numerous problems occur as a consequence, including protracted preparation and inefficient process planning. In the manufacture of structural components for aircraft, for example, process analysis and NC programming consume more than 70% of the time required for the entire process

The associate editor coordinating the review of this manuscript and approving it for publication was Bora Onat.

while the actual machining consumes less than 30% [2]. This characteristic also exists in the manufacturing stage of electronic product. Therefore, for the manufacturing of complex parts, the main loss of time is identified in the process planning field.

NC machining process reuse involves the use of existing digital design and manufacturing results to support the rapid design and manufacture of parts, which is an effective means to improve the efficiency of machining process planning [3]–[6]. Currently, various process reuse technologies, including group technology and machining process templates, have been widely studied. Thus Jong *et al.* [3] proposed an automatic process planning method that integrates feature recognition and group technology. However, this method groups the similar parts uses the part code, and its machining process reuse granularity is relatively extensive, which make it only applicable to reference reuse. Li *et al.* [7] proposed a geometric retrieval method for tool sequence reuse in mold NC machining, but it does not take fully into account the manufacturing semantic information, which is closely related to NC process planning; thus, the reuse value needs to be determined by the designer, and this method remains limited to reference reuse as well. Chen *et al.* [8] selected and adjusted the predefined macro process template manually and then, guided by the macro process, the machining method, cutting tool and cutting parameters of manufacturing feature are obtained by process rule inference to generate the machining process scheme of part. Li *et al.* [9] proposed a dynamic feature information model for the NC process design of aircraft structural parts. The method adaptively establishes the evolution state of each machining feature according to the typical process template selected by interaction, and then makes decision on the process parameters of the machining feature. Huang *et al.* [10] studied the NC process reuse method using 3D CAD model retrieval and CAM model (which is the program file generated by a CAM system, such as a.CATProcess file from CATIA or a.prt file from UG) data mining. Through the analysis and mining of existing process data, this approach reveals the NC process parameter-driven characteristics of similar features and, on this basis, allows for exploration of the inheritance mechanisms involved in implementing NC process reuse; then, the macro process plan for the part is realized through the reorganization and optimization of the reusable micro processes (i.e., those on feature/subpart level). As is apparent, this is a parameterized reuse method, the essence of which is bottom-up process planning. Although the above methods have received good results in improving the efficiency and quality of the NC process scheme, we also found that such bottom-up process planning methods usually rely on the assumption that the micro and macro processes are compatible. However, since the reusable NC process has the characteristics of multiple sources (from multiple parts), inherent heterogeneity (e.g., manufacturing resource heterogeneity and machining parameter variability) and local (i.e., at the feature or subpart level), the micro process and macro process are often difficult to be compatible, and require many considerable adjustment and optimization requirements in the form of manual intervention, thereby compromising the effectiveness of NC process reuse.

With the continuous improvement of intelligent computing algorithms and optimization algorithms in latest years, such as indicator-based evolutionary algorithm, parallel ant colony optimization and position disturbed particle swarm optimization, and the advantages of simple implementation and computational efficiency, it has been well applied in information system optimization. In the field of manufacturing, the NC machining process optimization approach has also been widely used in various stages of NC process planning, including machining sequencing [11]–[13], machining parameter selection [14]–[17], and tool path generation [18], [19]. Amid the ongoing evolution of intelligent NC process planning, optimization has been studied with respect to feature-based NC programming; thus Xu *et al.* [20], seeking to optimize the manufacture of aircraft parts, used the simulated annealing algorithm to obtain the shortest tool path. Zhang *et al.* [21] similarly optimized the cutting sequence in the NC machining of casing parts by establishing a mathematical model for the shortest tool path, dealing with the open and constrained traveling salesman problem using the tabu search algorithm. These methods, however, are intended mainly for the machining of independent features rather than of interacting features and have therefore been of limited use in improving the efficiency of the machining of parts overall. To overcome these limitations, Zheng *et al.* [22] proposed an optimized approach to machining process planning for complex parts with interacting features that begins with the maximum cutting depth and splitting the complex contour faces and then develops a genetic algorithm for the overall machining sequence, but this method is still inadequate for some complex structures. Liu *et al.* [23] used configuration spaces to represent and analyze the machining effect (i.e., undercut or overcut) and, through the iterative adjustment of the process scheme, updated and optimized the overall machining process; this method improves the efficiency of the process design but fails to give full consideration to machining parameters on the tool axis. Xu *et al.* [24] proposed an overall NC process reuse optimization method that combines an outer iteration, which generates an alternative process scheme, and an inner iteration, which creates an optimized machining operation precedence graph, thereby quickly yielding a complete process scheme for parts through reusable NC processes. Because this approach applies the existing optimization method directly, however, it cannot guarantee the validity and rationality of the resulting process scheme; for this reason, the difference between the process context of the reused NC processes and the machining requirements of the query parts—that is, the fact that the optimal reusable process scheme of a similar part is not necessarily optimal for the query part—is not considered. Based on these considerations, it appears that, once the reusable NC processes of machining features has been identified,

adaption and optimization of them are still necessary in order to improve the programming efficiency and ensure the rationality of the process scheme.

A. CONTRIBUTION

This paper presents an effective approach to optimizing the NC machining process for parts with complex pockets for NC process reuse in terms of resolving the problems discussed above. Its contributions can thus be summarized as follows:

- The proposed method takes into account the main parameters (i.e., cutting tool, cutting depth) of the machining region, thereby resolving the issues of (i) eliminating the heterogeneity and incompatibility among reusable processes for multiple parts through adjustment and optimization, (ii) extending the tool optimization range from single-layer to multi-layer on the level of the subpart, which can better reduce the number of tool changes and improve the machining efficiency, and (iii) optimizing the machining region under the constraint of the maximum cutting depth through dynamic selection of the cutting mode in a manner that makes full use of tool' machining capability and flexibility.
- The optimization with respect to the cutting tool and cutting depth is integrated into that of the tool path, which means that the problem of optimizing NC processes relating to parts can be considered from the perspective of the machining requirements for the query part. The hybrid ACO-TS algorithm also contributes to the optimization of the process scheme.
- The experiments on actual parts demonstrate the benefits of our optimization strategies; as the following discussion makes clear, our method outperforms others currently in use in terms of improving machining efficiency.

B. ORGANIZATION

The remainder of this paper is organized as follows. In section II, the problem description and the overview of our approach is presented. Section III gives the details of machining region optimization strategy, and Section IV describes optimization method of overall process path. Then in Section V, the experiments and discussion are provided. Finally, the research is concluded in section VI.

II. DESCRIPTION OF THE PROBLEM AND OVERVIEW OF OUR APPROACH

A. DESCRIPTION OF THE PROBLEM

With the ongoing accumulation of NC processes, reuse is an effective way of utilization based on similar structures to be found in the process instance repository. That is, features or subparts of multiple 3D CAD models are retrieved that have geometric and manufacturing semantics similar to those of the query part, and then an NC process scheme is created by reorganizing and optimizing the NC process segments of the various source structures. This bottom-up approach is associated with many problems, however, and

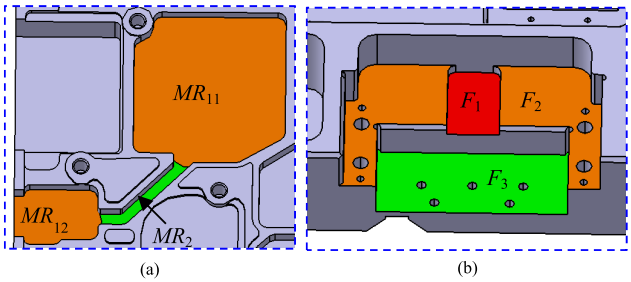

FIGURE 1. Examples of (a) a complex feature, *CF*, and (b) a subpart, S.

the performance of current process reuse is poor. In order to make clear the problems involved in NC process planning, we introduce here two key concepts, complex feature and subpart.

Definition 1: Complex feature (*CF*). A complex feature is defined as a machining feature that can be divided into multiple machining regions, each type of which corresponds to a tool that can cut them without interference. Further, the machining efficiency after division into multiple machining regions is greater than that when machining as a single region. As shown in Fig. 1(a), the feature C*F* is divided into three machining regions—MR_{11}, MR_{12} and MR_2, and MR_{11} and MR_{12}—that are manufactured with the same tool.

Definition 2: Subpart (*S*). A subpart is defined as a set of machining features connected with manufacturing-coupled relations that is independent of other features. The coupled relations include design interaction and manufacturing interaction [25]. Thus, for instance, pattern relation and datum relation belong to design interaction while dependent relation and adjacent relation belong to manufacturing interaction. Since design interaction is reflected mainly in the constraints on machining sequences at the macro level, the focus in this paper is on manufacturing interactions in the context of subparts. As shown in Fig. 1(b), the subpart *S* consists of three machining features—F_1, F_2, and F_3—of which F_1 depends on F_2 and F_3, and F_2 and F_3 have an adjacent relationship.

We now consider in detail the three issues listed in the previous section.

(i) **Incompatible NC process schemes.** At present, most of the features or subparts that show the greatest similarity to the query part among the search results are used, after appropriate modification, in designing NC process schemes. As a result of this focus, effective use is not made of instances of lower similarity. In fact, since the decision-making about processes occurs at the micro level, the influence of macro factors, such as overall topology and manufacturing relationship between features of the overall scheme, tends to be overlooked, while too little attention is paid to the fact that the NC processes associated with the query item's most similar features or subparts are not necessarily the most suitable from the perspective of the overall decision-making process.

(ii) **Frequent tool change.** For parts with complex features and subparts, there may be multiple cutting tool combinations (i.e. process solutions) for each machining feature, but they

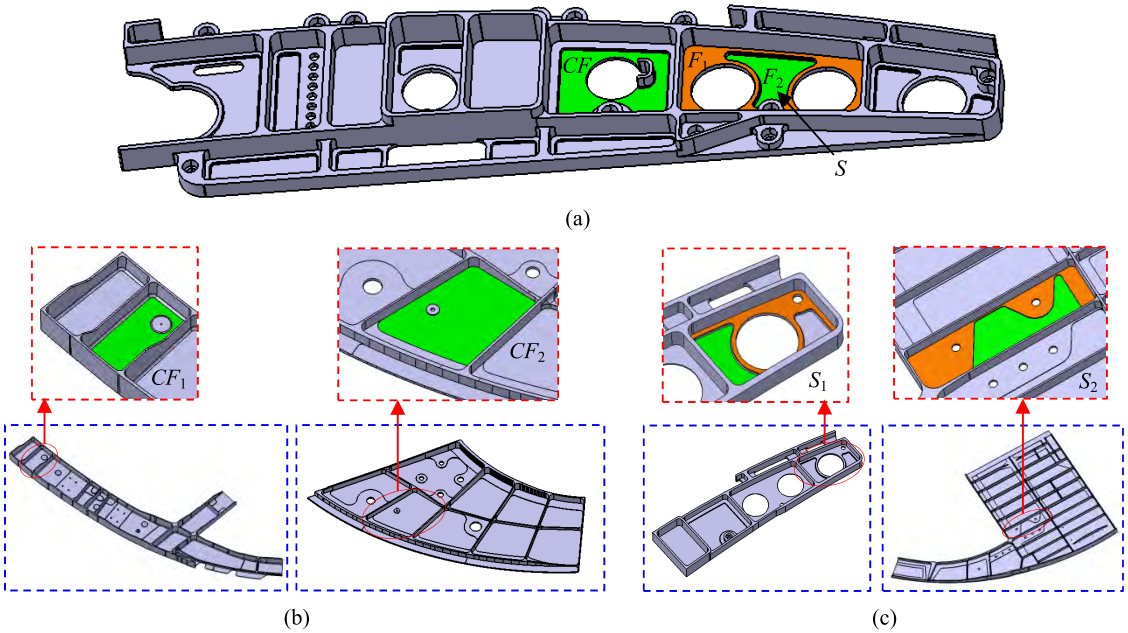

FIGURE 2. Sample of NC process reuse. (a) Complex feature and subpart of query part. (b) Reusable instances of complex feature *CF* from retrieval results (partial). (c) Reusable instances of subpart *S* from retrieval results (partial).

TABLE 1. Tool paths of the query part (partial).

Items	*CF*			*S*(F_1, F_2)		
	CF_1	CF_2	CF_3	S_1	S_2	S_3
NC process solution for subpart/feature	D14→D8	D16→D6	D8	D20(F_1)→ D16(F_2)→ D6(F_2)	D16(F_1)→ D16(F_2)→ D6(F_2)	D20→D6
Similarity	95.03%	81.71%	54.96%	83.65%	58.75%	36.87%
Machining time of *CF*/*S*	25.50s	23.93s	31.83s	65.31s	63.45s	63.62s
NC process scheme for part	Route 1: D14(*CF*)→D8(*CF*)→D20(F_1)→D16(F_2)→D6(F_2) Route 2: D16(*CF*)→D6(*CF*)→D16(F_1)→D16(F_2)→D6(F_2) Route 3: D16(*CF*)→D16(F_1)→D16(F_2)→D6(*CF*)→D6(F_2) …					

may be selected only from the perspective of individual features or subparts, again without proper consideration of the macro level. As a result, frequent tool change may be required during the machining process.

(iii) **Failure to optimize the machining region.** When the features in a subpart come together and the machining parameters obtained by the feature recognition technology are adopted for a NC process solution, many air-cutting paths may occur. In such a situation, the machining features obtained directly can only be used in the initial process scheme, for the geometrical parameters of the machining region, such as drive geometry and cutting depth, still need to be optimized before the process scheme can be finalized.

Taking the complex feature (*CF*) and the subpart (*S*) contained in the query part in Fig. 2 as an example, the preliminary NC process solutions were obtained from the retrieval of 3D CAD model [10] and NC process reuse. To illustrate the problem, we chose the three instances of greatest similarity among the NC process solutions and presented them in the order of tool combination. For the *CF*, an NC process solution of either CF_1: D14→D8 or CF_2: D16→D6 can be adopted. For the *S*, similar subparts, such as S_1 and S_2, were queried, yielding the corresponding NC process solution of D20→D16→D6, D16→D16→D6, which can be reused for *S*. As can be seen in Table 1, the machining efficiency of S_1, though this subpart is characterized by greater

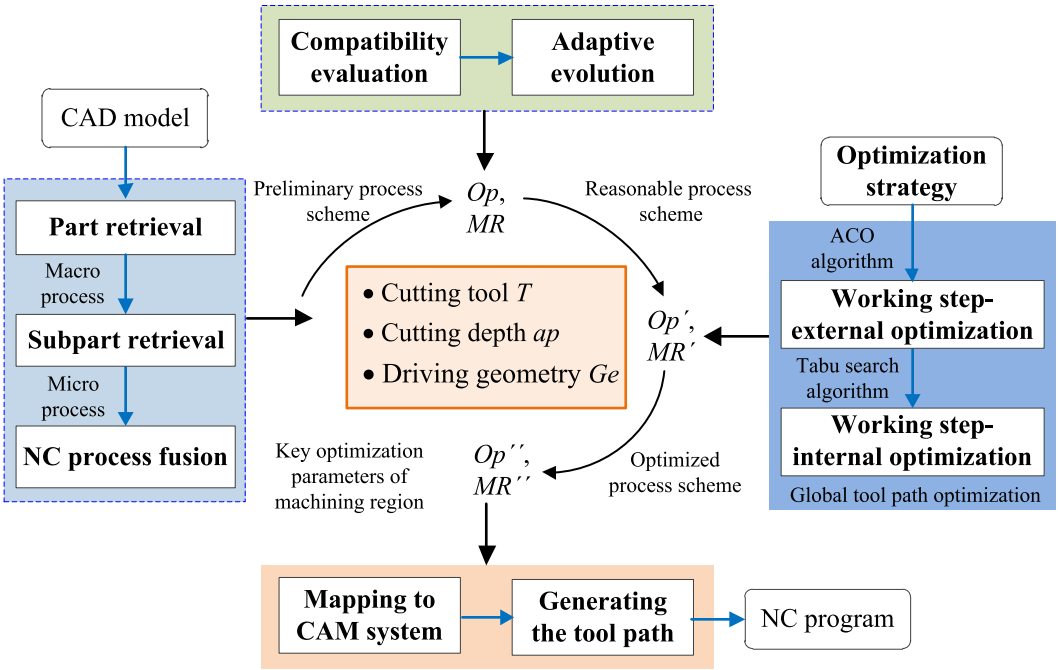

FIGURE 3. Framework for rapid NC programming driven by 3D CAD model retrieval (existing works are enclosed in the dotted lines).

similarity, is lower than that of S_2. Actually, the feasibility of the reusable NC process for the query part is an even more critical consideration, in light of which the machining parameters are set relatively conservatively for the given query part. In the machining process planning of the whole part, the tool path Route 1, following the traditional method, points to the NC process solution with the greatest similarity, again resulting in frequent tool change. Route 2, arrived at using the improved method, points to a set of process solutions with the greatest machining efficiency, thereby increasing overall efficiency, though the depth-first cutting mode still necessitates frequent tool change. Route 3, arrived at using the improved method and level-first cutting mode, results in increasing lifting times but avoids the problem of frequent tool change, making it the most efficient tool path. The traditional method of tool path optimization, which identifies the shortest path, therefore requires both selection of the appropriate similar instances for reuse and optimization of the cutting tools and the machining regions.

B. OVERVIEW OF OUR APPROACH

As currently conceived, interactive NC programming begins with the macro process scheme of a part, including the working procedures, working steps, and allowances, which is formulated through process analysis. The micro processes are then considered, including machining methods, cutting tools, and machining strategies, all with respect to the macro process. The result reflects both the programmer's habits and the designer's process intentions. Thus the rapid NC programming method driven by 3D CAD model retrieval involves identifying reusable macro and micro processes within the process instance repository and then combining the proper macro process with appropriate multi-source micro processes. As discussed in the previous section, further adaptation and optimization are necessary in order to make the process scheme practical. As shown in Fig. 3, then, rapid NC programming driven by 3D CAD model retrieval can be broken down as follows.

1. In the initial steps, 3D CAD model retrieval technology [6], [10] is used to obtain reusable macro and micro processes from multiple sources, and the preliminary NC process scheme is then generated by combining them. Next, the process scheme is evaluated for compatibility, that is, to determine whether the process requirements have been met and whether they support the kinds of adaptive changes [26] that can ensure the effectiveness and rationality of the scheme.
2. The corresponding optimization strategy is selected in order to reconstruct the machining region and optimize the cutting sequence across regions. The present study focuses on this aspect of the programming, which can usefully be subdivided into three steps:

(1) Machining region optimization strategy design. These strategies can take into account the cutting tool and cutting depth. First, the optimization strategy of the cutting tool is designed in accordance with the machining complexity of the complex features and the specific subpart. Next, the decision rules for the corresponding cutting mode are formulated so that the cutting depth and driving geometry of the machining region are optimal.

(2) Working step-external optimization. Assuming machining efficiency to be the goal of optimization, the sequence of working steps is optimized by taking advantage of the ant colony optimization algorithm in a global search. Meanwhile, the optimization strategies identified in the previous step are integrated into the process.

(3) Working step-internal optimization. Assuming the shortest path to be the goal of optimization and the result of the previous step to be the initial solution, the tool path is determined by taking the advantage of the tabu search algorithm in a local search that accounts for the cutting tool, machining region, and tool path.

3. The cutting sequence and optimized machining regions are then mapped into the CAM system, and one machining region is put into one operation accordingly, thereby completing the NC programming.

III. MACHINING REGION OPTIMIZATION STRATEGY

For a machining region, the corresponding machining operation settings include the cutting tool, the strategy, and the drive geometry. Among these parameters, the cutting tool and cutting depth are the key parameters to generate the tool path and directly affect the construction of the drive geometry. We therefore present our machining region optimization strategy in two parts: cutting tool optimization strategy and cutting depth optimization strategy.

A. CUTTING TOOL OPTIMIZATION STRATEGY

To solve the problem of selecting similar processes from multiple parts and the inconsistency of the associated parameters in the same process, it is necessary to optimize the cutting tools used in machining the complex features and subparts to meet the current process situation. The following is a detailed description of our cutting tool optimization strategy.

1) CUTTING TOOL OPTIMIZATION FOR MACHINING FEATURES

To achieve optimal machining, a complex feature is usually divided into various machining regions depending on the capability of the cutting tool and the geometry of the feature. Thus, each machining region can adopt different cutting tool, machining parameters, and pass strategy. As shown in Fig. 4(a), a complex pocket (P) is machined as a single region. Since the pocket has a narrow region and a small fillet, a smaller cutting tool, D4, is required to prevent overcut during the machining. As a consequence, the machining parameters are limited, that is, the smaller machining parameters (tool diameter $D_T = 4$mm, cutting width $a_e = 1$mm) are selected, which resulting that the low machining efficiency. Adopting the second NC process solution, P is divided into three machining regions, as shown in Fig. 4(b), for which cutting tools D8, D6, and D4 are used and more efficient machining parameters can be adopted according to the various types of tools. A pass strategy more suitable to the geometry of each region can also be adopted, thereby ensuring that the machining of the part is both competent and efficient. Thus, for example, the region machined by D8 has a cutting width of 2 mm, whereas that machined by D4 uses the zig-zag strategy and thus achieves higher machining efficiency owing to the relatively constant width.

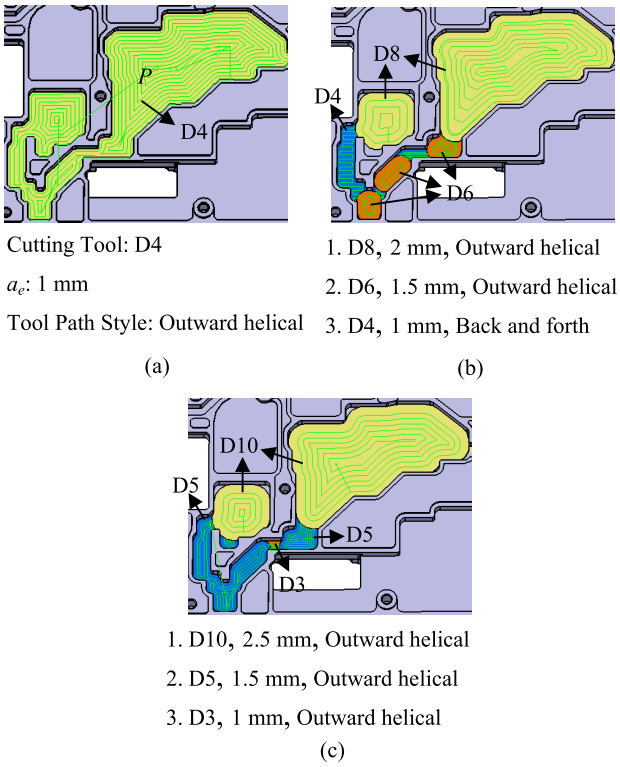

FIGURE 4. Sample of cutting tool optimization for machining feature. (a) NC process solution 1. (b) NC process solution 2. (c) NC process solution 3.

Each machining region of the complex feature division, then, may contain multiple machining sub-regions corresponding to specific geometric characteristics and machining strategies. A corresponding machining operation can be generated at the same time in the CAM system so that the complex features are expressed as

$$< F > ::= \bigcup_{k=1}^{N} MR_k$$
$$< MR > ::= < T > \cup < M_S > \cup < D_G >$$

where N is the number of the divided machining regions, MR represents the machining region, T is the cutting tool, M_S is the machining strategy (including the machining parameters, cutting mode, etc.), and D_G is the drive geometry (that is, the contour boundary of the machining region and is obtained using the algorithm in [26]).

The same CF could correspond to various tool combinations and divisions into regions based on similar instances obtained through the retrieval process, with all of the process solutions thus constituting the solution space of that CF. From the perspective of process optimization, it is still necessary to calculate the machining efficiency of each process solution so as to create a basis for subsequent decision-making relating

to process. Machining time is one indicator of machining efficiency and as such often plays a role in optimization. Therefore, this paper uses the machining time to optimize the combination of tools. The total machining time T_t is composed of the actual machining time T_m, the lifting time T_a, and the tool change time T_c, which can be represented as

$$T_t = T_m + T_a + T_c$$

where the actual machining and lifting time are related to the number of machining regions and tool change time to the number of tools used. Therefore, the total machining time can be calculated as

$$\begin{aligned} T_t &= \sum_{k=1}^{N} t_{mk} + (N-1)\, t_a + n_c \cdot t_c \\ t_{mk} &= \frac{A_k\, h\pi}{1000\alpha\, a_p\, v_k f_{kz} z} \\ t_a &= \frac{l}{v_a} + \frac{l}{v_r} \end{aligned} \tag{1}$$

where N is the number of the divided machining regions, t_{mk} is the machining time of the k-th machining region, t_a is the time of a single lifting, n_c is the number of tool changes, t_c is the time of a single tool change, L_k is the tool path length on the k-th machining region, f_k is the feed rate on the k-th machining region, A_k is the area of the k-th machining region, h is the machining depth, α is the proportional coefficient of the tool diameter occupied by the cutting part, a_p is the cutting depth, v_k and f_{kz} are the cutting speed and feed per tooth on the k-th machining region, z is the number of cutter teeth, l is the lifting height, v_a is the speed of rapid engage, and v_r is the speed of rapid retract.

As shown in Fig. 4(b) and 4(c), the two process solutions obtained from the search involve three tools and two tool changes. NC process solution 2 has two machining sub-regions using tool D8 and three each using D6 and D4. NC process solution 3 has two machining sub-regions each using D10 and D5 and one using D3. Calculating formula (1), the total machining time T_2 of NC process solution 2 is 29.4 s and the total machining time T_3 of NC process solution 3 is 23.3 s. It is clear that NC process solution 3 has higher machining efficiency and that the selected probability of the tool combination and division form is greater.

2) CUTTING TOOL OPTIMIZATION FOR SUBPARTS

Each machining feature involved in the subpart can be combined with a variety of cutting tool, which results in many different tool combinations for the machining of the subpart, but the number of used tools and the number of tool changes can reduced by merging during the subpart machining. Thus tool optimization in the context of subpart machining means solving problems associated with merging various machining features.

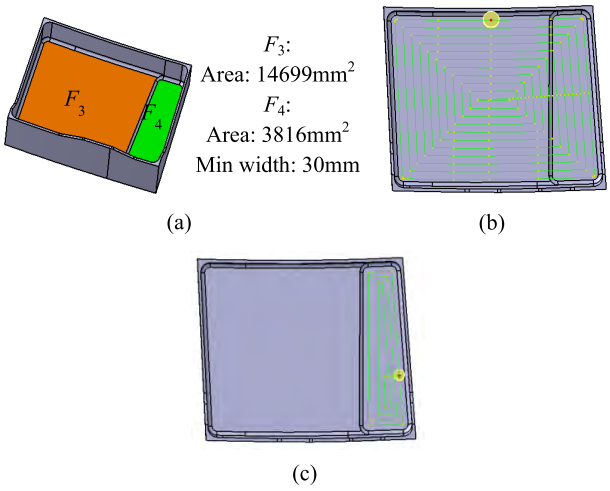

FIGURE 5. Sample of cutting tool merging for subpart machining. (a) Subpart 1. (b) Upper layer machining region and cutting tool. (c) Lower layer machining region and cutting tool.

a: CUTTING TOOL MERGING

While fewer cutting tools means less tool change time, the use of more tools can increase machining efficiency. Therefore, in the case of a small degree of influence on the machining efficiency of a large tool, it is possible to improve the efficiency by merging the tools used for the subparts, that is, by using the same small tool for features of the upper and lower layers and thereby reducing the number of tool changes. Since the machining time directly reflects the machining efficiency, it serves as a measure of whether the features of a subpart can be machined by the same cutting tool. Similarly, formula (1) is used to calculate the machining time. The specific formal representation is

$$\begin{aligned} &\text{if } T\ s_{t1} > T_{t2}, T_{t1} - T_{t2} < \delta R_1 > Rs_2, R_2 = R \\ &\text{then } R_1 = R_2 = R \end{aligned}$$

where R_1 and R_2 are the cutting tool radius of upper-layer and lower-layer machining regions, respectively, T_{t1} and T_{t2} are the total machining times of the upper and lower layer machining regions, respectively, and δ is a given threshold used to avoid diminished machining efficiency in the upper layer owing to tool adjustment that impacts the overall machining efficiency.

Fig. 5 shows an example of cutting tool merging for machining of a subpart. In the example, the machining area of F_3 = 14,699 mm^2 often involves use of tool D10 for roughing, while F_4 has a machining area of 3,816 mm^2 and a minimum width of 30 mm and often involves rough milling with D8. When F_3 and F_4 are in the same subpart, tool adjustment from D10 to D8 will not significantly reduce the machining efficiency of F_3(smaller than the threshold δ), according to the cutting tool merging rule introduced above, the tools for F_3 and F_4 can be merged and machined with tool D8, thereby reducing the tool change time. In addition, it should be noted that when there are more machining

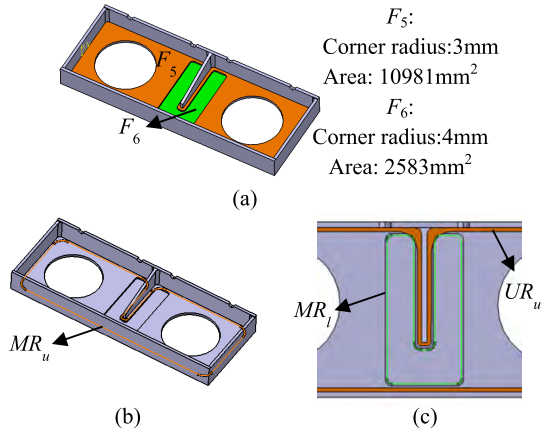

FIGURE 6. Example of cutting tool non-merging for subpart machining. (a) Subpart 2. (b) Upper layer machining region. (c) Lower layer machining region.

regions, the strategy can improve the machining efficiency more significantly.

b: CUTTING TOOL NON-MERGING

When a residual machining region remains after the upper-layer region has been machined, the machining of the lower-layer region is affected and the tool used for machining it cannot be merged with the one used for the upper region. In this case, the upper-layer residual region should be cleaned before the lower-layer region is machined, as follows:

$$\begin{aligned} &\text{If } UR_i \cap MR_j \neq \emptyset \\ &\text{Then } T(MR_i) \neq T(MR_j), \\ &\qquad T = \{T(MR_i), T_c(UR_i), T(MR_j)\} \end{aligned}$$

where UR_i is the residual region formed by the undercut after the first machining of the upper layer region, MR_j is the lower layer machining region, T is the cutting tool set used for machining the subpart, and $T_c(UR_i)$ is the tool used to remove the upper residual region.

As shown in Fig. 6, since the machining area of F_5 is large, the roughing stage uses cutting tool D12. However, with its corner radius being 3 mm, as can be seen in the figure, some residue remains after machining with D12, and there is a coupled relation between F_5 and F_6 in that the residue from the former affects the roughing of the latter. Therefore, based on the rules presented above, the roughing of F_5 and F_6 does not require optimization of the tools used by both.

B. CUTTING DEPTH OPTIMIZATION STRATEGY

After the cutting tool has been selected and the machining equipment and materials fixed, the cutting depth is determined based on the cutting mode for the machining region. Therefore, we first analyze the cutting mode of the machining region, and then according to the geometric relation between the features, the corresponding rules are defined to determine the cutting mode, thus supporting the optimization of the cutting depth.

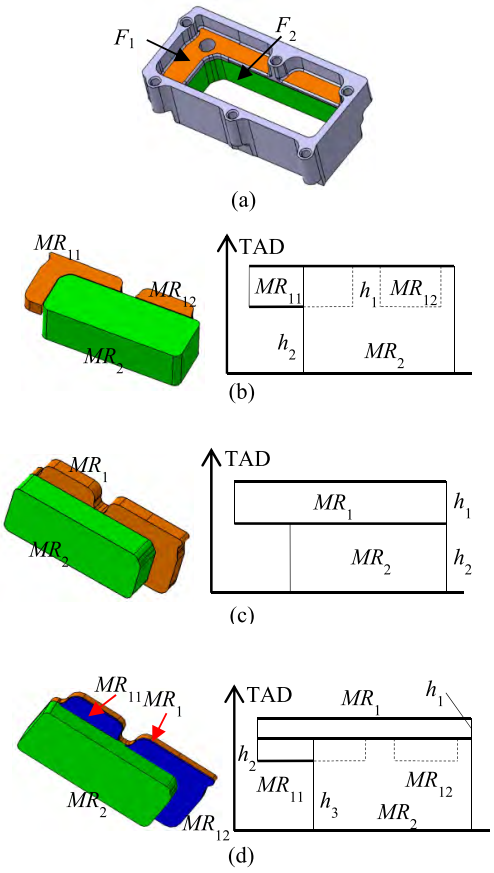

FIGURE 7. Category of cutting modes for subpart machining. (a) F_1 and F_2. (b) Depth-first. (c) Level-first. (d) Hybrid machining.

1) CUTTING MODE

For subpart machining, layering is usually performed at a constant cutting depth. Currently, three cutting modes are in common use, namely depth-first, level-first, and hybrid machining, as represented in Fig. 7.

a: DEPTH-FIRST

For interacting features, the depth-first cutting mode proceeds from processing the deeper to the shallower machining regions until all are completed. As shown in Fig. 7(b), F_2 is first machined into place, after which the two regions of F_1 are machined. The formalization of the machining region can thus be expressed as follows:

$$\begin{aligned} MR(F_i, F_j) &= (MR_i) \bigcup (MR_j) \\ MR_i &= (\bigcup_{k=1}^{N} SMR_{ik}, z_t, z_{bi}, \mathbf{n}) \\ MR_j &= (\bigcup_{k=1}^{M} SMR_{jk}, z_t, z_{bj}, \mathbf{n}) \\ z_{bi} &= z_t - n(ap_{\max}) \\ z_{bj} &= z_t - m(ap_{\max}) \end{aligned}$$

where MR_i and MR_j are the machining regions of F_i and F_j, SMR_{ik} and SMR_{jk} are the machining sub-regions of MR_i and MR_j, N and M are the number of machining sub-regions, z_t and z_b are the constrained bottom and top faces of the

feature, **n** is the tool axis feed direction of F_i and F_j, $ap_{\max}$ is the maximum cutting depth of the cutting tool, and n and m are the number of cutting layers required for F_i and F_j, respectively.

b: LEVEL-FIRST

The level-first cutting mode involves dividing all of the machining regions into various layers along the tool axis according to the cutting depth. The layers are fed one-by-one and the overall size of the features is approached gradually. As shown in Fig. 7(c), the upper layers of F_1 and F_2 are machined in a single operation, after which the remaining regions of F_2 are removed in another machining operation. This mode can thus be represented as

$$\begin{aligned} MR(F_i, F_j) &= (MR_i) \bigcup (MR_j) \\ MR_i &= (\bigcup_{k=1}^{N} SMR_{ik}, z_{ti}, z_{bi}, \mathbf{n}) \\ MR_j &= (\bigcup_{k=1}^{M} SMR_{jk}, z_{tj}, z_{bj}, \mathbf{n}) \\ z_{bi} &= z_{tj} \\ z_{bi} &= z_{ti} - n(ap_{\max}) \\ z_{bj} &= z_{tj} - m(ap_{\max}) \end{aligned}$$

c: HYBRID MACHINING

Hybrid machining, as the name suggests, involves combining the two cutting modes just discussed based on tool machining capacity. Generally speaking, the level-first mode is applied to the upper layer and the depth-first mode to discrete regions of the lower layer. Meanwhile, the machining region is optimized from bottom up based on the maximum cutting depth, and the whole region is divided up so that the tool can process as many regions as possible, thus effectively reducing its path length. As Fig. 7(d) indicates, F_2 can be extended up to a machining region, at which point F_1 can be reduced to a one layer feed and divided into three machining regions, MR_1, MR_{11}, and MR_{12}, as follows:

$$\begin{aligned} MR(F_i, F_j) &= (MR_i) \bigcup (MR_j) \bigcup (MR_l) \\ MR_i &= (\bigcup_{k=1}^{N} SMR_{ik}, z_{ti}, z_{bi}, \mathbf{n}) \\ MR_j &= (\bigcup_{k=1}^{M} SMR_{jk}, z_{tj}, z_{bj}, \mathbf{n}) \\ MR_l &= (\bigcup_{k=1}^{M} SMR_{lk}, z_{tl}, z_{bl}, \mathbf{n}) \\ z_{bi} &= z_{tj} = z_{tl} \\ z_{bi} &= z_{ti} - n(ap_{\max}) \\ z_{bj} &= z_{tj} - m(ap_{\max}) \\ z_{bl} &= z_{tl} - (ap_{\max}) \end{aligned}$$

For parts with larger numbers of machining regions, the depth-first cutting mode is adopted in order to reduce the lifting times for the tool path, and the machining efficiency is correspondingly higher. Compared with the depth-first mode, the level-first mode displays better mechanical properties, for it can ensure uniformity in the machining of materials and thus reduce machining deformation. The level-first mode is thus used preferentially in the machining of the thin-walled parts. Hybrid machining, again, combines the advantages of both modes.

2) RULES FOR CHOOSING THE CUTTING MODE

The choice of cutting mode is determined by the actual geometry and process characteristics of the machining parts. The area and volume of the machining region in a subpart directly affect the selection of the cutting mode and machining parameters and consequently the subpart's machining efficiency. Thus a subpart S that contains machining features F_u and F_l exists in a kind of parent-child relationship with them. If F_u is in the upper layer and its machining area is much smaller than that of F_l, the level-first mode is used; thus the portion of the region in F_u can be machined in F_l, thereby reducing the time required to process one layer region. In this context, we introduce the quantitative index volume-area radio (VAR) as a means to support automatic decision-making regarding cutting mode; it can be expressed as

$$VAR = (H_u/H_l)/(A_u/A_l)$$

where H_u and H_l are the height of machining regions of F_u and F_l, respectively, A_u and A_l are the area of machining regions of F_u and F_l, respectively.

Based on the calculated VAR, the following rules can serve to select the cutting mode that yields the optimal cutting depth parameters.

Rule 1: When the machining area of the upper feature of a subpart exceeds that of the lower feature, that is, when $VAR<\delta$, the depth-first cutting mode should be used. In general, this mode is preferred because it has the highest machining efficiency. When VAR is far less than δ, direct machining in place can simplify the tool path, thereby indirectly improving the machining speed.

Rule 2: When the machining area of the lower feature exceeds that of the upper feature, that is, when $VAR>= \delta$, the level-first or hybrid machining mode should be used. Simultaneously, the coplanar regions of the cutter axis can be combined in the machining. When VAR is far greater than δ, the machining efficiency can be improved by making full use of the tool machining capacity so as to reduce the tool path layers. In addition, the number of regions and operations increases during the machining, though this increase does not affect use of the cutting tools.

Rule 3: Residue from the upper machining can interfere with the lower machining, or, when the upper and the lower regions are combined in machining, their number increases markedly. Under such circumstances, regardless of the size of VAR, the machining features of the subpart cannot be combined; that is

$$UR_u \cap MR_l \neq \emptyset \text{ or } \mathrm{Num}\,(SMR'_u) - \mathrm{Num}\,(SMR_u) >= 2$$

where Num(•) is the number of the machining sub-regions and SMR_u and SMR'_u are the machining sub-regions of the upper feature before and after optimization, respectively.

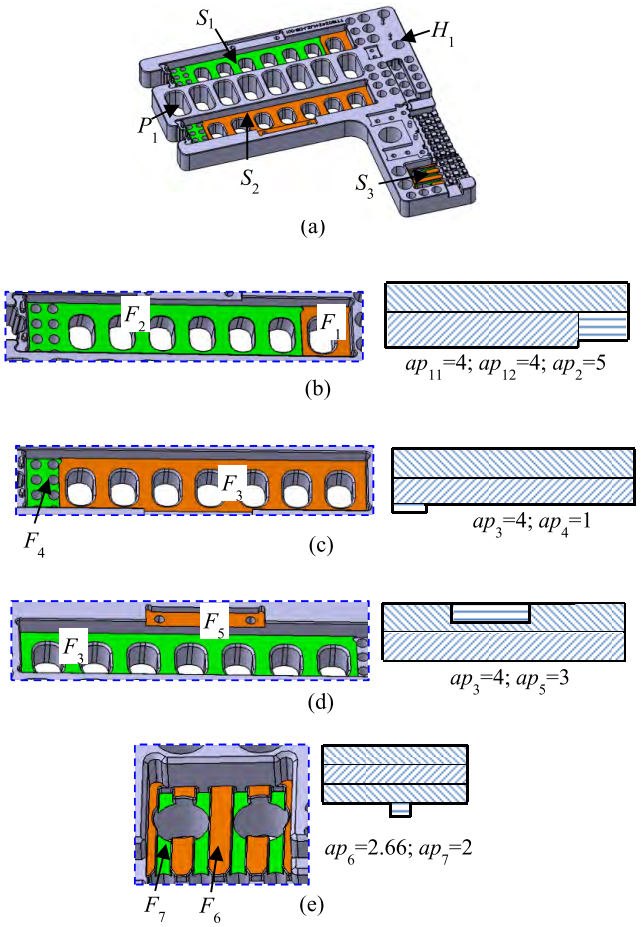

FIGURE 8. Sample of cutting-depth optimization for subpart machining. (a) Part I. (b) Cutting mode and cutting depth of S_1. (c) Cutting mode and cutting depth of S_2(F_3 and F_4). (d) Cutting mode and cutting depth of S_2(F_3 and F_5). (e) Cutting mode and cutting depth of S_3.

At this point, for a residual machining region in the upper feature, it is necessary to increase the working steps in order to avoid the interference of the lower in the machining process. However, when the number of machining regions increases greatly after combination, the original process solution is retained so as to avoid complicating the tool path or increasing the lifting times, both of which would affect machining quality and efficiency.

Fig. 8 shows an example of cutting depth optimization for a subpart that includes 78 independent features (e.g., P_1, H_1) and 6 subparts (e.g., S_1, S_2, S_3). The height and area of feature F_1 in subpart S_1 are $H = 8$ mm, $A = 690$ mm^2 and of feature F_2 are $H = 9$ mm, $A = 3{,}900$ mm^2. S_2 consists of features F_3($H = 8$ mm, $A = 4{,}260$ mm^2), F_4($H = 9$ mm, $A = 450$ mm^2), and F_5($H = 3.25$ mm, $A = 400$ mm^2). Since the *VAR*s of S_1 and S_2 (F_3 and F_4) are 5.02 and 0.09, respectively, hybrid machining is selected for S_1 based on **Rules 1** and **2** (here, $\delta = 1$), and the upper machining region can be divided in order to improve machining efficiency. In accordance with the tool selected, $ap_{\max} = 5$ mm. Thus, machining efficiency is improved for S_1 by machining region MR_1, a cutting depth 4mm of op_1, machining region MR_2, a cutting depth 4mm of op_2, machining region MR_3, and a cutting depth 5mm of op_3. Moreover, S_2 (F_3 and F_5) retains a level-first mode and can be machined using either the depth-first or level-first mode. Considering that a machining region has a larger corner with the level-first mode, the depth-first mode can be used for S_2 (F_3 and F_5) with the corresponding cutting depths of 4 mm and 3 mm. The lower layer of S_3 contains multiple machining regions; and since, based on **Rule 3**, the upper machining region cannot be split, the level-first mode is still used. In addition, S_3 calls for a smaller tool, and its $ap_{\max}$ is much smaller; the cutting depth is 2.66 mm and 2mm.

IV. GLOBAL TOOL PATH OPTIMIZATION APPROACH

At present, optimization of the machining path focuses mainly on the cutting sequence for given machining regions, while there has been little study of the combination of cutting tool and tool path. In fact, the machining regions depend on the tools selected, for which reason the combination of the cutting tools is a key factor relating to the tool path. Therefore, the proper manner in which to combine the cutting tool and the cutting sequence is the core problem in the achievement of efficient machining.

A. OPTIMIZATION MODEL

The machining strategy determines the frequency of tool change during the manufacture of subparts; thus, for example, the depth-first mode can reduce lifting and air-cutting times. However, the tools used in machining the upper and lower regions may differ, thereby increasing the number of tool changes. This number should accordingly be taken into consideration first when optimizing the cutting sequence. For tool changes between the machining regions, the calculation of machining time when optimizing the sequence (T_{tc}) can be expressed as

$$T_{tc} = \sum_{i \in V, j \in V} a_{ij}\, b_{ij}\, t_c \tag{2}$$

where V is the geometry of machining region, a_{ij} is 1 when the j-th machining region is machined after the i-th region and otherwise 0, b_{ij} is 1 when the j-th and i-th machining regions use different tools and otherwise 0, and t_c is the time required for the tool change.

After determining the cutting tool, optimization of its cutting sequence mainly takes into account the influence of the tool path on the machining efficiency. In the constant machining region, the total length of the tool path is a function of the cutting sequence and the engage and retract positions. In particular, when the machining region of the part is fairly complicated, the various cutting sequences differ considerably from the total tool path length generated by the engage and retract positions, among which the machining parameters of each tool are certain. Therefore, optimization of the cutting sequence and the engage and retract positions reduces the length of the total tool path and thus the machining time while improving the machining efficiency. The total path

length consists of the path length for the cutting, for the non-cutting engage and retract positions, and for the lifting between the machining regions. Thus, the machining time in cutting sequence optimization (T_{tr}) can be calculated as

$$T_{tr} = \sum_{i \in W, j \in W} a_{ij}\left(\frac{L_{mi}}{v_m} + \frac{L_{ari}}{v_{ar}} + \frac{L_{tij}}{v_t}\right) \tag{3}$$

where W is the set of machining regions, a_{ij} is 1 when the j-th machining region is machined after the i-th region and otherwise 0, L_{mi} is the tool path length of the i-th machining region, L_{ari} is the length of engage and retract path of the i-th machining region, L_{tij} is the length of the lifting path between the i-th and jth machining regions, v_m is the cutting speed, v_{ar} is the engage and retract speed, and v_t is the lifting speed.

In the whole cutting sequence optimization process, the former mainly considers the influence of tool change, which can be regarded as the optimization of cutting sequence between working steps. And the latter mainly considers the influence of tool path on machining efficiency, which can be regarded as the optimization of cutting sequence within the working steps. This level of optimization is therefore essentially a combinatorial problem. If the working step and the machining region are represented together as a node, optimization of the cutting sequence can be approached as a special constrained traveling salesman problem, the objective function of which can be described as follows:

$$\begin{aligned} &\min f(x) \in \{f(x_1), f(x_2), \cdots\cdots, f(x_{n!-1})\} \\ &\text{s.t.} \begin{cases} x \in D = \{x_i \,|\, 1 < i \leq n! - 1\}; \\ T_f = \{T_1, T_2, \cdots\cdots, T_m\}, 1 \leq m \leq n; \\ MR(T_k) = \{T_k, T_{k+1}, \cdots\cdots, T_{k+l}\}, 1 \leq l \leq n, \\ 1 \leq k \leq m. \end{cases} \end{aligned} \tag{4}$$

where n is the number of machining regions, x is a cutting sequence of these machining regions, T_f is the set of cutting tools corresponding to the cutting sequence x, and $MR(T_k)$ is the set of machining regions machined by T_k. If the adjacent regions are machined by the same tool, they can be combined in the same working step. If the regions are not adjacent, they can be regarded as distinct working steps that use the same tool.

B. OPTIMIZATION MODEL SOLUTION

Viewed from the perspective of the geometric characteristics and process analysis of query parts, optimization of the cutting sequence optimization involves the combination of working steps and features. Currently, many swarm intelligence algorithms are available for solving the problem associated with the optimization, including the ant colony optimization (ACO), tabu search (TS), genetic algorithm (GA), and simulated annealing (SA) algorithm. The ACO algorithm in particular has strong global search ability and thus has been widely used for process optimization, though it is subject to local convergence. The TS algorithm is a global, step-by-step search algorithm better suited to identifying the optimal local solution, though it has a strong dependence on the initial solution. In light of these strengths and weaknesses, we propose a hybrid ACO and TS optimization algorithm as a means to improve the quality of searches. This algorithm consists of two main stages. First, for optimization between working steps with respect to the influence of tool changes on machining efficiency, the ACO algorithm quickly identifies an optimized or approximate optimized solution. This solution to the ACO algorithm serves in turn as the initial solution to the TS algorithm, which, taking into account the influence of the tool path on machining efficiency, is applied to narrow further the search for the optimal solution.

1) FITNESS FUNCTION

The working step-external optimization reduces the machining time and improves machining efficiency mainly by reducing the number of tool changes. However, the tool path is indispensable for calculating the time consumed by the entire machining process. Therefore, to prevent the overall optimal solution from being filtered out in the first optimization stage, the tool-changing time serves as the main optimization objective and the machining path as the auxiliary objective. In this way, the optimization of the working steps is regarded as a multi-objective optimization problem, and the reciprocal is used as the fitness function. At the same time, the greater the fitness, the greater the probability of selection. The fitness function of a process scheme is accordingly expressed as

$$F_{tc} = \frac{1}{\omega_1 T_{tc} + \omega_2 T_{tr}} \tag{5}$$

where ω_1 and ω_2 are eights between 0 and 1 satisfying the conditions (1) $\omega_1 + \omega_2 = 1$ and (2) $\omega_1 > \omega_2$.

Different from the working step-external optimization, the working step-internal optimization concentrates on the machining regions that use the same tool and on reducing machining time by shortening the tool path. There are, therefore, no tool changes involved in this kind of optimization. The reciprocal of the machining time required by the path is taken as the fitness function, which also conforms to the rule that the fitness correlates positively with the probability of being selected, and can be expressed as

$$F_{tr} = \frac{1}{T_{tr}} \tag{6}$$

2) WORKING STEP-EXTERNAL OPTIMIZATION

The working step-external optimization in the previous stage serves mainly to identify multiple global optimal solutions quickly. In doing so, the ACO algorithm is first used to conduct a quick search. For complex parts, the input machining region set may come from one of the many methods of segmentation of complex features by region. Therefore, to begin with, the time consumed in machining for each process solution of complex features is calculated in the ways introduced in the previous section. Next, in accordance with

TABLE 2. Working step-external optimization algorithm.

Algorithm: ACO algorithm
Input: the set of machining regions MR_S={MR_i},1≤i≤n
Output: the set of optimal tool paths P_S={$\boldsymbol{MR}[n]_j$},1≤j≤m
(1) Begin
(2) Initialize F_{tc}, m, $iter_{max}$
(3) Initialize Φ
(4) Copy MR_S to set S
(5) While $iter$ <$iter_{max}$ || P_S=ϕ
(6) For every ant in the colony k
(7) While S≠ϕ
(8) Select the machining region that the ant visits next according to the probability MR_i
(9) Delete the machining region MR_i in S
(10) Optimize and update the tool information of the visited machining regions according to the tool optimization rules in the previous section,
(11) End while
(12) End for
(13) Calculate the maximum fitness for this iteration F_{iter}
(14) Determine if F_{iter} needs an update based on F_{tc}
(15) Update Φ
(16) Iterations $iter$=$iter$+1
(17) End while
(18) Return P_S
(19) End

the principle that the machining time should be shortened and the selection probability increased, the least time-consuming process solution is selected as the preliminary scheme and segmentation of the machining regions is performed. Finally, the alternative process solution is chosen iteratively, and the ACO algorithm is repeated in order to obtain several better solutions.

Table 2 shows the working step-external optimization based on the ACO algorithm in which the pheromone model is $\Phi(\tau_1, \tau_2, \ldots, \tau_n)$, with n being the number of the machining regions, τ_i the number of pheromones accumulated in machining region i, and a larger value meaning greater probability of selection for inclusion in the tool path. The first step in the optimization involves initialization of the Φ and the relevant variables F_{tc}, representing the current search for the global optimal solution, m, representing the number of ants in the colony, and $iter_{max}$, representing the maximum iteration time of the algorithm. In the next steps, the solution space is searched by iteration, a complete machining route is constructed for each ant in the process of searching, and the machining region is optimized and updated according to the tool used for the subpart. After optimization of the machining region is complete, the optimal solution of the iteration F_{iter} is calculated, and F_{tc} is assessed to determine whether updating is necessary; if so, Φ is recalculated in accordance with the values of F_{tc} and F_{iter}. Finally, the tool path corresponding to F_{iter} is stored in the set P_S until the better solutions are found, at which point the algorithm ends.

The proposed ACO algorithm includes four key factors in the optimization process, namely pheromone initialization, calculation of transition probability, fitness update, and pheromone model update, each of which is described in the following discussion.

(1) Pheromone initialization

The number of each pheromone Φ is limited to an interval $[\tau_{\min}, \tau_{\max}]$. Limiting the number of each pheromone in this way can prevent uneven distribution of pheromonoes, stagnation of the search process, and recourse to the local optimum. During the initialization of the pheromone model, the initial value of all the pheromones on the vertices is $\tau_{\max}$.

(2) Calculation of transition probability

When an ant moves from a machining region op_i to a possible machining region op_j, its transition probability can be calculated according to the concentration of the pheromone and the length of each tool path as

$$P_{i,j}^{k}(t) = \frac{\left[\tau_{i,j}(t)\right]^{\alpha}\left[\eta_{i,j}(t)\right]^{\beta}}{\sum_{t\in N_i^k}\left[\tau_{i,j}(t)\right]^{\alpha}\left[\eta_{i,j}(t)\right]^{\beta}} \tag{7}$$

where N_i^k is the set of machining regions that ant k has not yet accessed, $\tau_{\mathrm{i,j}}(t)$ is the amount of the pheromone on the path (i, j) at moment t, $\eta_{\mathrm{i,j}}$, (t) is the reciprocal of the path length (i,j), α and β are the weights on the probability of the influence of the pheromone and the tool path length, respectively, and $\alpha < \beta$.

(3) Fitness update

When any ant k constructs a complete tool path, that path can be further optimized according to the cutting tool optimization strategy for the subpart. The more accurate fitness functions are then calculated on the basis of the optimized tool path, which is in turn used to determine whether the fitness should be updated. The specific judgment method is as follows:

$$F_{tc} = \begin{cases} F_{iter}, & \text{if } F_{tc} < Fs_{iter} \\ F_{tc}, & \text{otherwise} \end{cases} \tag{8}$$

(4) Pheromone model update

In an iterative process, when all of the ants have constructed a complete tool path, the optimal solution F_{iter} for this iteration is calculated according to the fitness of the tool path constructed by each individual ant. Then, based on the value of F_{iter}, a determination is made as to whether F_{tc} should be updated. If so, the pheromone model is updated according to formula (9) and (9).

$$\begin{aligned} \tau(v_i) &= \rho \cdot \tau(v_i) + \Delta\tau(v_i) \\ \Delta\tau(v_i) &= \begin{cases} \dfrac{1.5}{1 + |F_{tc}| - |F_{iter}|}, & v_i \in F_{iter} \\ 0, \quad \text{otherwise} \end{cases} \end{aligned} \tag{9}$$

where ρ is the pheromone persistence rate and is < 1.

TABLE 3. Working step-internal optimization algorithm based on TS.

Algorithm: TS algorithm
Input: optimal solution x found by the ACO algorithm
Output: the optimal path x^*
(1) Begin
(2) Set x as the initial solution, $x=x^*$
(3) Initialize the tabu table $t=\phi$, aspiration criteria $A(s,x)= F_{tr}(x^*)$, and iteration times $iter$ =0
(4) While N(x)\t$\neq\phi$ && $iter<iter_{max}$
(5) If $F_{tr}(s_L(x))=Opt\{F_{tr}(s(x)),s(x)\in N(x)\}$ && $F_{tr}(s_L(x))>A(s,x)$
(6) $x= s_L(x)$
(7) else if $F_{tr}(s_L(x))=Opt\{F_{tr}(s(x)),s(x)\in N(x)\backslash t\}$
(8) $x= s_k(x)$
(9) End if
(10) If $F_{tr}(x)< F_{tr}(x^*)$
(11) $x^*=x$
(12) $F_{tr}(x^*)=F_{tr}(x)$
(13) $A(s,x)=F_{tr}(x^*)$
(14) End if
(15) $iter$++
(16) End while
(17) Return x^*
(18) End

3) WORKING STEP-INTERNAL OPTIMIZATION

In the working step-internal optimization, the tool path generated by the ACO algorithm can serve as a good initial solution, and the tabu search (TS) algorithm can serve as input in performing a local search for the purpose of improving further the solution space and obtaining the final optimization solution. Since the cutting depth and machining region are related to the selected tool, the various cutting sequences generated by the ACO algorithm affect both the initial machining region and tool path. Therefore, prior to overall optimization, the individual machining regions need to be optimized according to the cutting depth optimization strategy described in the previous section. Combined with the actual machining process requirements, the TS algorithm has been improved so as to be more suitable for the NC process optimization. The specific process for working step-internal optimization based on TS is shown in Table 3.

In this process, a current solution (initial solution x), a neighborhood $N(x)$, and several candidate solutions $\{s_L(x)\}$ in the neighborhood are determined. If the best candidate solution corresponding to the target value $C(s_L(x))$ is better than the ''best solution'' state $A(s, x)$, its tabu features are initially ignored and the current solution and the ''the best solution'' state are replaced. Next, the corresponding object is added to the tabu table and the term of each object therein is modified. If no candidate solution is found, the non-constrained optimal state $N(x)\backslash t$ is selected as the new candidate solution and the superiority and inferiority of the current solution are ignored. Finally, the corresponding object is again added to the tabu table and the term of each object therein is modified. This iterative search process is repeated until the stopping criterion is met.

There are six main parts of the working step-internal optimization algorithm based on TS, which are now discussed in turn.

(1) Expression of the solution

The solution to the problem is usually expressed as a mathematical function. In the TS, however, the fitness function is used to represent the solution, which also serves as the objective function. In our algorithm, the fitness function is finally transformed into F_{tr}. In addition, the initial solution x makes use of a feasible solution obtained when the ACO algorithm converges.

(2) Neighborhood and movement of neighborhood

In the function optimization problem, the neighborhood movement can be defined as a given step size and moving direction; in the combinatorial optimization problem, on the other hand, it can be defined as a sequence of permutation. In our algorithm, the neighborhood movement is constrained in the same step; that is, the cutting sequence between the two machining regions within the same tool can be replaced. The neighborhood $N(x)$, which is formed by the current solution x, represents a set of solutions that can be achieved through a defined neighborhood movement.

(3) Tabu table

The tabu table is used to prevent cycle search; in general, the movement, the moving component, and the fitness function are regarded as the tabu objects; in this paper, however, only the first and last of these are regarded as the tabu objects.

(4) Selection strategy

The selection strategy ensures that the TS algorithm has the ability to jump out of the local optimal solution. Thus, in each moving step of the current solution x, the current solution always moves to the optimal solution that is not taboo in the neighborhood $N(x)$; that is:

$$\text{If } F_{tr}(s_L(x)) = Opt\{F_{tr}(s(x)), s(x) \in N(x)\backslash t\}$$
$$\text{then } (x = s_L(x))$$

where $s_L(x)$ is the optimal solution which is not taboo in the neighborhood $N(x)$.

(5) Aspiration criterion

The aspiration criterion $A(s, x)$ is a value depending on s and x. If the candidate solution $s(x)$ in the neighborhood is greater than the aspiration criterion, then $s(x)$ is not restricted by the tabu table; that is:

$$F_{tr}(s(x)) > A(s, x)$$

when the above condition obtains, even if $s(x) \in t$, x can still move towards $s(x)$. $A(s, x)$ generally selects the optimal value that can be reached. The aspiration criteria and taboo strategies together constitute the two core movement rules of the tabu search algorithm.

(6) Stop criterion

The stop criterion of the tabu search algorithm generally takes one of three forms, either the maximal iteration time,

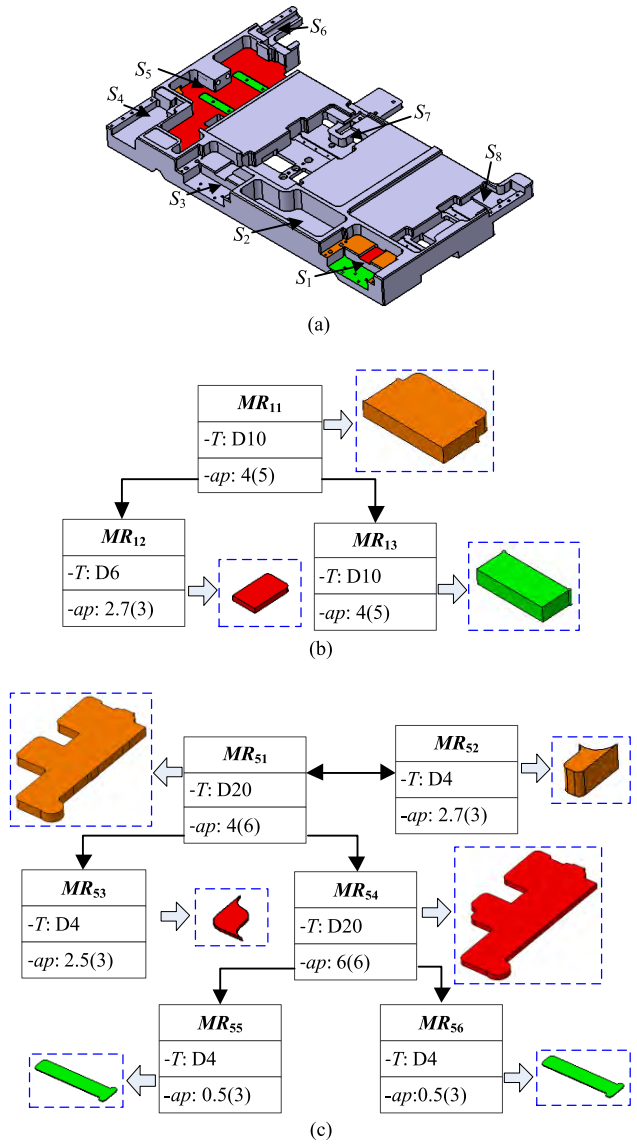

FIGURE 9. Calculation for machining region optimization strategy. (a) Part1. (b) Optimization result of S_1. (c) Optimization result of S_5.

the satisfactory solution, or the maximal tabu frequency. In this paper, the maximal iteration time serves as the stop criterion.

V. EXPERIMENTS AND DISCUSSION

To verify the feasibility and effectiveness of our approach, we developed a prototype system for NC machining process optimization of parts with complex pockets for NC process reuse on the platforms Microsoft Visual Studio 2008 and CATIA V5 R21 component application architecture (CAA). The test was executed on a PC with Intel Core i3 CPU 3.40GHz and 4 GB of memory.

A. MACHINING REGION OPTIMIZATION CALCULATION CASE

Fig. 9 shows the calculation of the machining region optimization for Part 1, which consists of 30 pockets and 8 subparts. Subpart S_1 is composed of three machining features and S_5 of four, one of which is complex feature. As can be seen in Fig. 9(b), the area of the lower layer region is greater than that of the upper, though the difference is minimal, as is the improvement in machining efficiency when the machining regions are combined. In addition, combination of the regions complicates the tool path to the detriment of the machining speed. Thus, considering all of these factors together, the depth-first cutting strategy best suits S_1. Moreover, since the machining regions are generated directly from the recognized machining features, the tool path and machining parameters of the initial process scheme are insufficiently optimized. As can be seen in Fig. 9(c), modification of the initial process scheme involves adjustment of three parts of the optimized scheme for S_5. These adjustments are (1) division of complex features into two machining regions, MR_{51} and MR_{52}, which are machined with tools D20 and D4, respectively; (2) making full use of the tool machining capacity, that is, MR_{54} contains a part of the upper region in order to reduce the number of machining layers in MR_{51}; and (3) combination of cutting tool, D6 in the initial solution is the best choice for machining the smaller regions in S_5, such as MR_{52} and MR_{53}, in order to improve the machining effect. However, because MR_{55} and MR_{56} can only use D4 owing to limited tool accessibility, MR_{52} and MR_{53} are eventually adjusted to accommodate this tool so as to reduce the number of tool changes.

Table 4 presents the results of the statistical analysis for the optimization strategy for Part 1. In order to focus on the impact of the strategy on machining efficiency, this case involved only optimization of the machining results in the subpart; the machining optimization between the subparts is discussed in the following section. As can be seen in Table 4, optimization of the cutting sequence and the cutting tool reduced the number of tools from 6 to 4 and the number of tool changes by half, with D20 and D4 being used for most of the machining. As the use times of the maximum cutting depth parameter increased, the optimized process scheme became more advantageous in terms of maximizing the tool machining capacity. All subparts in the initial process scheme used the level-first cutting mode. The method proposed here, however, adopts various optimization strategies according to the geometric characteristics of the subpart in order to achieve dynamic optimization effects. Finally, through optimization of the cutting tool and cutting depth, the overall machining time for the part was reduced from 988.36 s to 825.04 s and the efficiency increased by 16.25%. The proposed optimization strategy thus has the potential to improve machining efficiency.

B. GLOBAL OPTIMIZATION CASE OF PART AND RESULT ANALYSIS

The optimization strategy calculation can yield a better solution for the machining region and cutting tool for Part 1. In the following discussion, Part 1 serves as an example of the effectiveness of global optimization of the part.

TABLE 4. Analysis of calculation for machining region optimization strategy.

Items for comparison	Preliminary process scheme			Optimized process scheme with our approach		
Cutting tool	D32, D20, D10, D8, D6, D4			D32, D20, D10, D4		
The number of machining regions corresponding to the tool	2, 11, 7, 4, 2, 14			2, 13, 6, 16		
Number of tool changes	22			11		
Use times of maximum cutting depth	3			8		
Cutting mode and use times	Depth first	Level first	Hybrid machining	Depth first	Level first	Hybrid machining
	-	20	-	8	8	4
Machining time(s)	988.36			825.04		
Improvement in efficiency	16.52%					

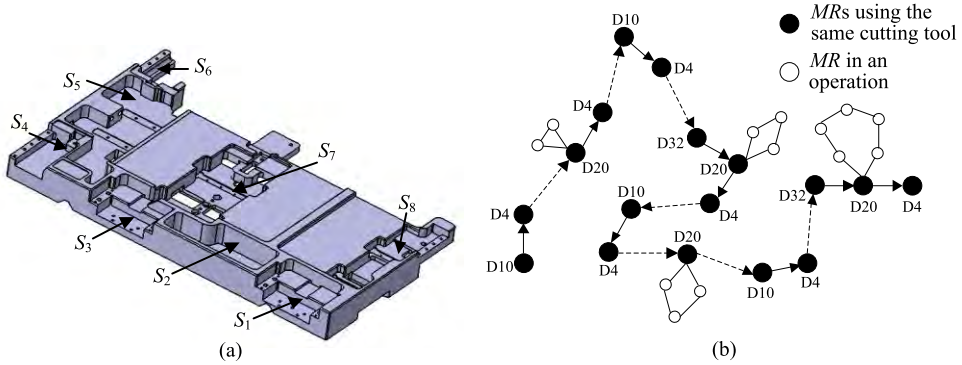

FIGURE 10. Global optimization of Part 1. (a) Part 1. (b) The preliminary process scheme for Part 1.

TABLE 5. Length of tool path between the 8 subparts.

Subpart to Subpart	S_1	S_2	S_3	S_4	S_5	S_6	S_7	S_8
S_1	0	75.5	184.3	285.2	271.3	333.9	166.4	88.1
S_2		0	108.8	209.8	201.1	273.0	109.3	114.8
S_3			0	80.7	111.0	201.4	94.5	201.6
S_4				0	76.7	163.9	160.1	292.4
S_5					0	95.6	115.5	255.5
S_6						0	167.6	294.6
S_7							0	140.1
S_8								0

As mentioned, Part 1 consists of 8 subparts, includes 37 machining regions, and is machined with 4 cutting tools, as can be seen in Fig. 10, which makes clear the frequent tool changes required in the non-optimized tool path of the preliminary process scheme. It is, therefore, necessary to optimize the process scheme from the perspective of the global machining of the part. In order to achieve better optimization results, we tested various parameter values. For the ACO algorithm, we set the weights α and β to 1.5 and 2, the pheromone continuation rate ρ to 0.7, the maximum iteration time at 300, and the number of ants (m) to half the number of points. For the TS algorithm, we set the tabu table length to 3 and the maximum iteration time to 100.

TABLE 6. Comparison of the optimization results for three tool paths.

No.	Tool path	Minimum path length	Number of tool changes
1	S_1-S_1-S_2-S_3-S_3-S_4-S_4-S_5-S_5-S_6-S_6-S_7-S_7-S_7-S_8-S_8-S_8	745.0	16
2	S_1-S_3-S_4-S_6-S_7-S_8-S_8-S_7-S_5-S_2-S_3-S_4-S_5-S_6-S_7-S_8-S_1	1951.9	3
3	S_7-S_8-S_8-S_7-S_5-S_6-S_6-S_5-S_7-S_8-S_1-S_3-S_4-S_4-S_3-S_1-S_2	1535.3	6

TABLE 7. Comparison of optimization and non-optimized approaches.

Cutting tool	optimization approach		non-optimized approach	
	Path length(mm)	Lifting times	Path length (mm)	Lifting times
D(T)=32	12,084.2	48	34,385.6	44
D(T)=20	10,390.5	11	12,369.3	18
D(T)=8	3,598.6	10	3,901.0	10
Total	26,073.3	69	50,655.9	72

After planning the tool path, we calculated its length in the machining region. The lengths of the moving tool path among the 8 subparts are presented in Table 5.

Turning now to working step-external optimization, Table 6 presents a comparison of the optimization results for various tool paths that takes into account the number of tool changes and the length of the tool path. The tool path length of Part 1 could be optimized to 745mm, but the number of tool changes was large. In tool path 2, the number of tool changes could be reduced to 3, but the length of this path would be some 3 times that of tool path 1. Therefore, considering the number of tool changes and the length of the tool path, we found tool path 3 to be optimal for Part 1.

For working step-internal optimization, the first consideration is optimizing the path between the subparts; thus, for tool D20, the best path was $S8$-$S7$-$S5$-$S2$. The next consideration is the general constraints (e.g., the machining of MR_1 must precede that of MR_2 because of an accessibility constraint in the machining of MR_1 in relation to the access faces of MR_2) [24]. Finally, the optimized tool path is obtained based on the two constraints.

Fig. 11 shows another sample, the more complex part Part 2, which we use here to illustrate the feasibility and effectiveness of the global part optimization method. Part 2 is an aircraft structural with thin-wall features, so, in order to reduce deformation, the level-first cutting mode is generally used to process the regions within. Thus, after the

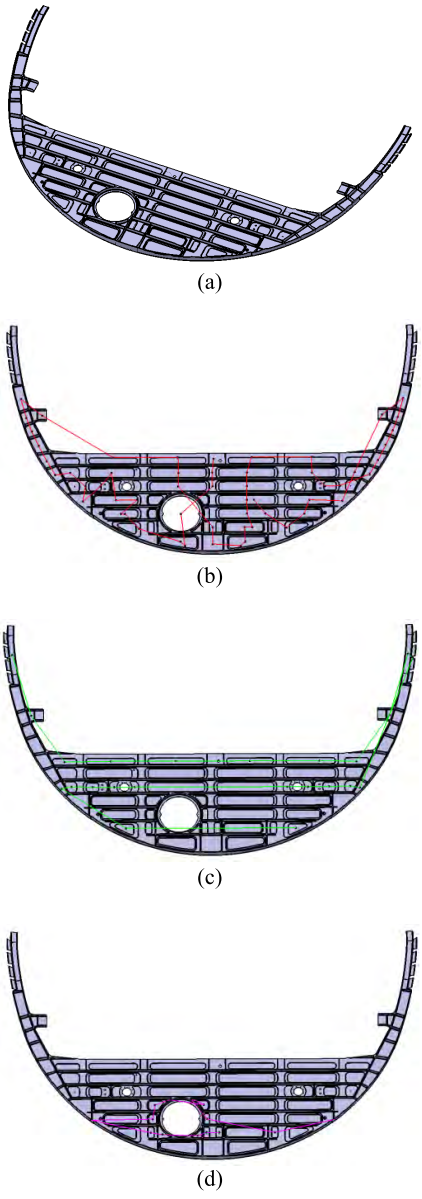

FIGURE 11. Global optimization of Part 2. (a) Part 2. (b) Optimized tool path with tool D32. (c) Optimized tool path with tool D20. (d) Optimized tool path with tool D8.

cutting tool optimization, we used only cutting tools D32, D20, and D8, proceeding in order from large to small. The red line in Fig. 11(b) represents the optimized tool path for the 73 regions machined with D32, and the green line in Fig. 11(c) represents the optimization result for the 26 regions machined with D20. After machining with the large cutting tools D32 and D20, we removed the remaining small regions and residual regions with D8, as shown by the pink line in Fig. 11(d).

Table 7 presents a comparison of the results for the tool paths in machining regions with tools D32, D20, and D8 when they were and were not optimized using our method. Although the lifting times increased after optimization of the regions machined with D32, the length of the tool path

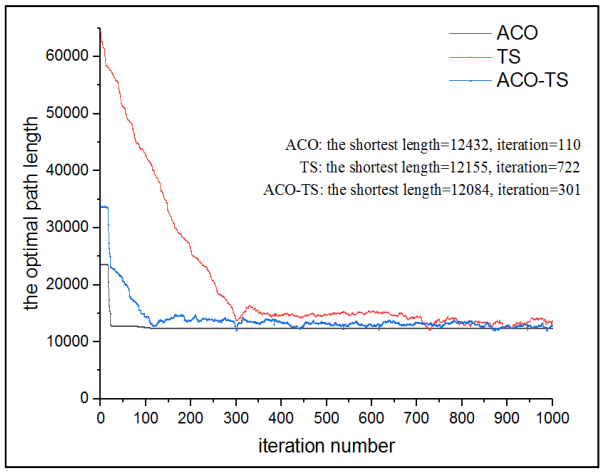

FIGURE 12. Comparison of global optimization methods for Part 2.

decreased markedly. This means that, in order to minimize the total tool path, lifting times can be increased. In optimizing the regions machined with D20 and D8 so as to shorten the tool path, then, it appears that more complicated machining situations experience a more significant effect. In general, we reduced the total tool path length by 24,582.6 mm and the cutter-lifting times by two-thirds compared with the non-optimized cutting sequence method. We accordingly conclude that our global optimization method can effectively shorten tool path length, reduce cutter-lifting times, and thereby decrease machining time and improve machining efficiency.

Fig. 12 presents a comparison of the tool path optimization results for the working step D32 Rough Milling stage using either the ACO algorithm, the TS algorithm, or the hybrid ACO-TS algorithm. We had to set numerous parameters for the experiment, and the main parameter settings were consistent with the Part 1 optimization test. In order to observe the iterative results better, we set the maximum iteration time in the experiment to 1,000. As Fig. 12 shows, the ACO algorithm quickly found the optimal solution after only 110 iterations and was able to converge quickly. The TS algorithm, on the other hand, converged very slowly. Our method found the optimal solution after 301 iterations, and the iteration time is short; therefore, our global optimization method of the parts discussed in this paper yielded greater optimization efficiency than the other two methods. In addition, the iterative results demonstrate that the optimal path calculated using our method was the shortest. The TS algorithm, on the other hand, found the optimal solution more easily than the ACO algorithm. We conclude, in any case, that our global optimization method performed better than the other methods.

C. PROTOTYPE SYSTEM AND MACHINING SIMULATION

Fig. 13 illustrates the prototype system for NC machining process optimization. The steps for the function are as follows: (1) selection of feasible NC process solutions from

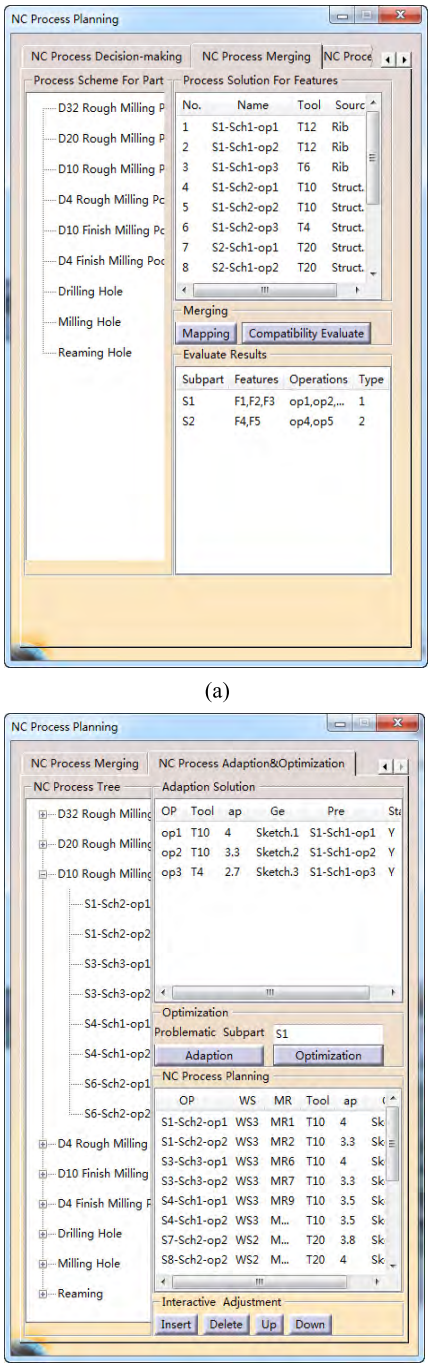

FIGURE 13. Prototype system for NC machining process optimization. (a) Preliminary process scheme generation. (b) Process scheme optimization.

various similar subparts and mapping of them onto a reusable macro process of the part that can generate a preliminary process scheme based on the query part, as shown in Fig. 13(a); (2) evaluation of the compatibility of the process scheme for completeness and feasibility and display of the results of the analysis in a list, on which each result contains the problematic subpart, the associated machining features and operations, and the type of problem (e.g., overcut or frequent

TABLE 8. Comparisons of our approach with existing approaches.

Method	Cutting tool optimization		Cutting depth optimization		Tool path optimization		Flexibility	Feature interaction consideration	Elimination of incompatibility
	Optimization range	Tool change time	Optimization range	Tool capacity utilization	Cutting mode	Optimization algorithm			
Liu et al. [23]	-	More	Maximum cutting depth	Middle	Level-first	GA	Low	Y	N
Zheng et al. [24]	Single	More	-	Low	Level-first	-	Low	Y	N
Ahmad et al. [28]	Single	More	-	Low	Level-first	GA	Low	N	N
Our approach	Multi	Less	Dynamic	High	Hybrid	ACO-TS	High	Y	Y

tool changes), after which either the problematic subpart is replaced with an alternative process solution or the cutting sequence and machining parameters are adjusted; and, finally, (3) optimization of the preliminary process scheme, as shown in Fig. 13(b). In this third step, either the tool path in the same working step is optimized automatically or the interactive adjustment is used to add or delete the machining operation or to adjust the sequence and add it to the NC process tree, after which the adjusted tree is mapped to the CAM system so as to yield a sequence of machining operations for the query parts.

Generally speaking, the machining simulation can be conducted so that it reflects the actual NC machining and represents the final part. If the simulation result proves feasible and free of errors, the designed process is available for actual NC machining. Accordingly, in order to verify the effectiveness of our approach, we conducted a simulation based on CATIA, as depicted in Fig. 14. The result of the machining simulation of the stock shown in Fig. 14(a) for the optimal NC process scheme for S_5 is presented in Fig. 14(b)-(f). The analysis of the final part made clear that no material or gouge remained, meaning that this optimized NC process scheme achieved satisfactory machining quality with no overcuts. Comparing Fig. 14(g) with Fig. 14(h), in which each color represents a distinct cutting tool, it is evident that our method uses fewer tools than other methods; in addition, as shown in Table 4, it requires less machining time. The simulation experiment thus indicated that our NC process optimization approach has practical application value because it can satisfy the requirements of actual NC machining.

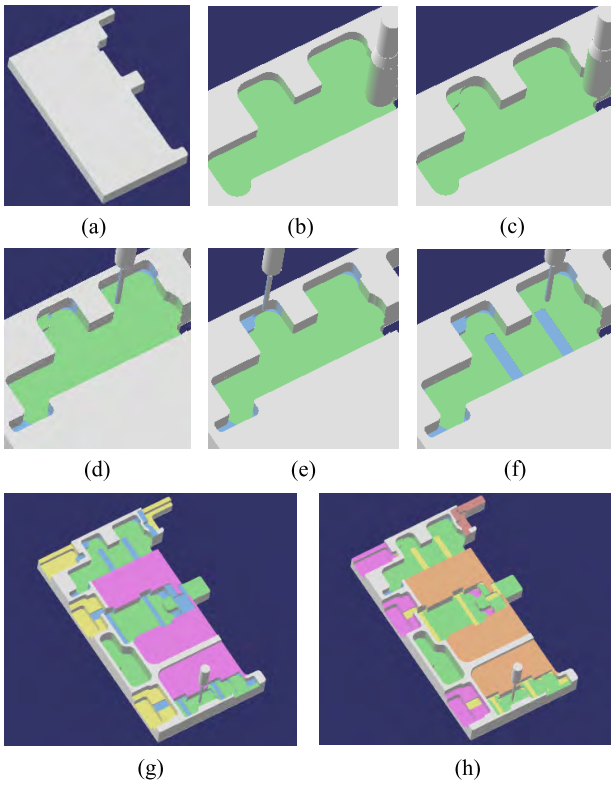

FIGURE 14. The machining simulation. (a) The stock. (b) MR_{51} of S_5. (c) MR_{54} of S_5. (d) MR_{52} of S_5. (e) MR_{53} of S_5. (f) MR_{55} and MR_{56} of S_5. (g) The final result with the optimized approach. (h) The final result with the non-optimized approach.

D. DISCUSSION

Table 8 presents a comparison of our approach with some existing approaches. These current methods are usually optimized for tool combinations of complex features and only take into account the machining of the single-layer region. Our approach, by contrast, extends the optimization range to the subpart in order to support multi-layer machining regions. Other optimization methods also fail to consider the order in which the cutting tools are used between the machining features and thus do not reduce the number of tool changes. With regard to cutting depth, Liu *et al.* [23] proposed a detailed detection and optimization method for the interaction regions in the radial direction, but their method is less concerned with the interaction between the machining features in the axial direction and, as a result, the machining capability of the tools is limited. Zheng *et al.* [22] reconstructed the machining regions between the interacting features with the

maximum cutting depth, but the utilization efficiency of the tool machining capacity for this method is still far from satisfactory. In our approach, on the other hand, because it is based on the maximum cutting depth constraint according to the geometric characteristics of the interacting features, the selection of cutting is conducted so that the tool machining capacity can be more fully utilized. Both of these teams of researchers adopted the level-first cutting mode for their optimization methods. Our method, however, based on the geometric characteristics of the part, dynamically selects a reasonable cutting mode so as to arrive at the process scheme with the shortest tool path and thus offers greater flexibility. Our method also takes advantage of hybrid optimization, combining the ant colony and tabu search algorithms to find the best path. Further, unlike the cutting tool selection method proposed by Ahmad *et al.* [27], our method takes into account interactions among features and, again, extends the optimization range from single-layer tool optimization of complex features to multi-layer tool optimization of subparts. At the same time, by eliminating the heterogeneity and incompatibility associated with reusable processes involving multiple parts, our method can, unlike other methods, solve the problem of excessive manual intervention in the later stage of process reuse-based NC process planning.

VI. CONCLUSION AND FUTURE WORK

In this paper, we have presented an effective NC machining process optimization approach for parts with complex pockets for NC process reuse. In our method, the cutting tool and cutting depth of the machining region are first optimized by making full use of the tool's machining capacity and avoiding air-cutting. Next, the cutting sequence of the machining regions is optimized from a macro perspective in order to obtain an efficient process scheme. Finally, a prototype system based on CATIA serves to verify the effectiveness of the proposed approach.

A number of the issues raised by our research merit further exploration: (1) at present, the method only optimizes the cutting depth of the machining parameters related to the geometry of the machining region, and the optimization of other machining parameters can also improve the machining efficiency. For example, the spindle speed and the feed rate are optimized from the deformation view in combination with the rigidity calculation; (2) the optimization method is mainly applied for the roughing stage, and can be further used for other machining stages, such as optimizing the machining region contour of the interacting feature in the finishing stage; (3) the current optimization goal is mainly machining time, and energy consumption can be added as another optimization goal to form a multi-objective optimization problem, and thereby obtain a high-efficiency and low-energy NC process scheme.

REFERENCES

[1] J. Zhou, P. Li, Y. Zhou, B. Wang, J. Zang, and L. Meng, "Toward new-generation intelligent manufacturing," *Engineering*, vol. 4, no. 1, pp. 11–20, 2018.

[2] R. F. Harik, W. J. E. Derigent, and G. Ris, "Computer aided process planning in aircraft manufacturing," *Comput.-Aided Des. Appl.*, vol. 5, no. 6, pp. 953–962, 2008.

[3] W. R. Jong, P.-J. Lai, Y. W. Chen, and Y.-H. Ting, "Automatic process planning of mold components with integration of feature recognition and group technology," *Int. J. Adv. Manuf. Technol.*, vol. 78, nos. 5–8, pp. 807–824, 2015.

[4] H. Zhang *et al.*, "Modularization of feature information for marine diesel engine parts," in *Proc. 2nd Int. Conf. Electron. Mech. Eng. Inf. Technol.*, 2012, pp. 923–926.

[5] A. Cardone, S. K. Gupta, A. Deshmukh, and M. Karnik, "Machining feature-based similarity assessment algorithms for prismatic machined parts.," *Comput.-Aided Des.*, vol. 38, no. 9, pp. 954–972, 2006.

[6] B. Huang *et al.*, "An effective retrieval approach of 3D CAD models for macro process reuse," *Int. J. Adv. Manuf. Technol.*, 2018. doi: 10.1007/s00170-018-2968-8.

[7] Z. Li, X. Zhou, W. Liu, and C. Kong, "A geometry search approach in case-based tool reuse for mould manufacturing," *Int. J. Adv. Manuf. Technol.*, vol. 79, nos. 5–8, pp. 757–768, 2015.

[8] S. Chen, G. Zheng, M. Zhou, B. Du, and H. Chu, "Process-scheme-driven automatic construction of NC machining cell for aircraft structural parts," *Chin. J. Aeronaut.*, vol. 26, no. 5, pp. 1324–1335, 2013.

[9] Y. Li, X. Liu, J. X. Gao, and P. G. Maropoulos, "A dynamic feature information model for integrated manufacturing planning and optimization," *CIRP Ann.*, vol. 61, no. 1, pp. 167–170, 2012.

[10] R. Huang, S. Zhang, C. Xu, X. Zhang, and C. Zhang, "A flexible and effective NC machining process reuse approach for similar subparts," *Comput.-Aided Des.*, vol. 62, pp. 64–77, May 2015.

[11] S. Kafashi, "Integrated setup planning and operation sequencing (ISOS) using genetic algorithm," *Int. J. Adv. Manuf. Technol.*, vol. 56, nos. 5–8, pp. 589–600, 2011.

[12] F. Musharavati and A. M. S. Hamouda, "Simulated annealing with auxiliary knowledge for process planning optimization in reconfigurable manufacturing," *Robot. Comput.-Integr. Manuf.*, vol. 28, no. 2, pp. 113–131, 2012.

[13] Q. Hu, L. Qiao, and G. Peng, "An ant colony approach to operation sequencing optimization in process planning," *Proc. Inst. Mech. Eng., B, J. Eng. Manuf.*, vol. 231, no. 3, pp. 470–489, 2017.

[14] X. Liu, Y.-P. Ding, C. Yue, R. Zhang, and X. Tong, "Off-line feedrate optimization with multiple constraints for corner milling of a cavity," *Int. J. Adv. Manuf. Technol.*, vol. 82, nos. 9–12, pp. 1899–1907, 2016.

[15] H. Xu and D. Li, "Modeling of process parameter selection with mathematical logic for process planning," *Robot. Comput.-Integr. Manuf.*, vol. 25, no. 3, pp. 529–535, 2009.

[16] C. Peng, H. Du, and T. W. Liao, "A research on the cutting database system based on machining features and TOPSIS," *Robot. Comput.-Integr. Manuf.*, vol. 43, pp. 96–104, Feb. 2017.

[17] C. Liu, Y. Li, X. Zhou, and W. Shen, "Interim feature-based cutting parameter optimization for aircraft structural parts," *Int. J. Adv. Manuf. Technol.*, vol. 77, nos. 1–4, pp. 663–676, 2015.

[18] Z. Zhai, Z. Lin, and J. Fu, "HSM toolpath generation with capsule-based region subdivision," *Int. J. Adv. Manuf. Technol.*, vol. 97, nos. 1–4, pp. 1407–1419, 2018.

[19] H. Abdullah, R. Ramli, and D. A. Wahab, "Tool path length optimisation of contour parallel milling based on modified ant colony optimisation," *Int. J. Adv. Manuf. Technol.*, vol. 92, nos. 1–4, pp. 1263–1276, 2017.

[20] J. Xu, G. Zheng, B. Du, H. Chu, and F. Wu, "Mathematical model and algorithm of toolpath optimisation on aircraft structural parts," *Int. J. Prod. Res.*, vol. 52, no. 4, pp. 1142–1149, 2014.

[21] C. Zhang, F. Han, and W. Zhang, "A cutting sequence optimization method based on tabu search algorithm for complex parts machining," *Proc. Inst. Mech. Eng., B, J. Eng. Manuf.*, vol. 233, no. 3, pp. 745–755, 2019.

[22] Z. Zheng, Q. Wang, G. Zheng, and J. Zhu, "An optimal approach to manufacturing planning for complex prismatic parts with interacting feature," *Int. J. Adv. Manuf. Technol.*, vol. 94, nos. 1–4, pp. 585–597, 2018.

[23] X. Liu, Y. Li, and L. Tang, "A dynamic feature–based operation planning method for 2.5-axis numerical control machining of complex structural parts," *Proc. Inst. Mech. Eng., B, J. Eng. Manuf.*, vol. 229, no. 7, pp. 1206–1220, 2015.

[24] C. Xu, S. Zhang, R. Huang, B. Huang, and X. Li, "NC process reuse-oriented flexible process planning optimization approach for prismatic parts," *Int. J. Adv. Manuf. Technol.*, vol. 87, nos. 1–4, pp. 329–351, 2016.

[25] R. Huang, S. Zhang, X. Bai, and C. Xu, "Multi-level structuralized model-based definition model based on machining features for manufacturing reuse of mechanical parts," *Int. J. Adv. Manuf. Technol.*, vol. 75, nos. 5–8, pp. 1035–1048, 2014.
[26] H. Rui and Z. Shusheng, "An effective adaptive dynamic evolution computing approach of roughing process for part with complex pockets," *Int. J. Adv. Manuf. Technol.*, vol. 96, nos. 9–12, pp. 3279–3293, 2018.
[27] Z. Ahmad, K. Rahmani, and R. M. D'Souza, "Applications of genetic algorithms in process planning: Tool sequence selection for 2.5-axis pocket machining," *J. Intell. Manuf.*, vol. 21, no. 4, pp. 461–470, 2010.

BO HUANG received the B.S. degree from Harbin Engineering University, China, in 2013, and the M.S. degree from Northwestern Polytechnical University, China, in 2014, where he is currently pursuing the Ph.D. degree with the School of Mechanical Engineering. His research interests include CAD/CAPP/CAM, data-driven manufacturing, and 3D CAD model retrieval.

SHUSHENG ZHANG received the B.S. and M.S. degrees from Northwestern Polytechnical University, China, in 1980 and 1984, respectively, and the Ph.D. degree from the University of Havre, France, in 1991. He is currently a Professor with the School of Mechanical Engineering, Northwestern Polytechnical University. His research interests include digital design and manufacturing, reverse engineering, and 3D CAD model retrieval.

RUI HUANG received the B.S. degree in aircraft manufacturing engineering and the M.S. degree in aeronautics and astronautics manufacturing engineering from Northwestern Polytechnical University, China, in 2009 and 2010, respectively, and the Ph.D. degree from the School of Mechanical Engineering, Northwestern Polytechnical University, China, in 2016. He is currently an Assistant Professor with the College of IOT Engineering, Hohai University, China. His research interests include CAD/CAM, 3D CAD model retrieval, and computer graphics.

XIULING LI received the M.S. degree in mechanical manufacturing and automation from the Lanzhou University of Technology, China, in 2013. She is currently pursuing the Ph.D. degree with the School of Mechanical Engineering, Northwestern Polytechnical University, China. Her research interests include knowledge-based design and intelligent manufacturing systems.

YAJUN ZHANG, photograph and biography not available at the time of publication.

JIACHEN LIANG, photograph and biography not available at the time of publication.